Pergamon

Solid State Communications, Vol. 101, No. 3, pp. 187–192, 1997

0038–1098/97 $17.00+.00

PII: S0038-1098(96)00531-5

MAGNETIC PROPERTIES OF THE ONE-DIMENSIONAL $Ca_3Co_2O_6$

S. Aasland,[a] H. Fjellvåg[a] and B. Hauback[b]

[a]Department of Chemistry, University of Oslo, N-0315 Oslo, Norway
[b]Institutt for energiteknikk, N-2007 Kjeller, Norway

(*Received* 12 *April* 1996; *in revised form* 2 *September* 1996; *accepted* 9 *September* 1996 *by J. Kuhl*)

The magnetic properties of $Ca_3Co_2O_6$ have been studied by magnetic susceptibility and neutron diffraction methods from 5 K to room temperature. Magnetic ordering occurs below 24 ± 2 K. Above 80 K, the Curie–Weiss law is followed and an effective magnetic moment of $5.7 \pm 0.2\,\mu_B$ was found. The magnetic structure of $Ca_3Co_2O_6$ has been refined from Rietveld analysis of powder neutron diffraction data at 10 K. The one-dimensional chains in $Ca_3Co_2O_6$ were found to have alternating low magnetic moment ($0.08 \pm 0.04\,\mu_B$) for the octahedral cobalt and high magnetic moment ($3.00 \pm 0.05\,\mu_B$) for the trigonal prismatic cobalt ions. Magnetic moments close to zero were indicated in the **ab**-plane. $Ca_3Co_2O_6$ is ferrimagnetic at low temperatures, with ferromagnetic ordering dominating within the Co–O chains. In high magnetic fields, above around 2.7 MA m^{-1}, a field-induced transition from ferrimagnetic to ferromagnetic structure occurs, implying turning of the spins in one chain. Copyright © 1996 Elsevier Science Ltd

Keywords: A. magnetically ordered materials, C. Crystal structure and symmetry, E. neutron scattering.

1. INTRODUCTION

The compound $Ca_3Co_2O_6$ has been known for a long time [1, 2], however the structure was solved only recently. $Ca_3Co_2O_6$ crystallizes in space group *R-3c* with $Z = 6$ (hexagonal setting) and $\mathbf{a} = 907.93(7)$ and $\mathbf{c} = 1038.1(1)$ pm at 298 K [3]. The rhombohedral structure has distinct one-dimensional features with Co–O chains along the **c**-axis where the Co-atoms form alternating face sharing coordination polyhedra of trigonal prisms and octahedra. Each chain is surrounded by six similar chains, at a distance of 524 pm. Owing to the face-sharing, very short Co–Co distances appear within the chains, i.e. 259.5 pm. Distinctly different Co–O distances were found for the octahedra and trigonal prisms [3]. The same structure type has been reported for Sr_3NiIrO_6, where the one-dimensional chains consist of alternating face-sharing octahedral IrO_6 and trigonal prismatic NiO_6 [4]. Complex magnetic transitions as a function of temperature and a singlet ground state below 15 K were reported for Sr_3NiIrO_6 [4]. The present study reports on the magnetic properties and magnetic structure of $Ca_3Co_2O_6$ based on magnetic susceptibility and neutron diffraction data collected at low temperatures.

2. EXPERIMENTAL

Powdered polycrystalline $Ca_3Co_2O_6$ was prepared by a citrate method as previously described [3]. Starting materials of $CaCO_3$ (Merck, p.a.) and $Co(CH_3COO)_2\,4H_2O$ (>99%, Fluka) were dissolved in citric acid (reagent grade, Sturge biochemicals) and destilled water at 100°C. The clear citrate gel was dehydrated at 450 K and most of the carbonaceous species was removed by incineration at 720 K for a few hours. The sample was finally heat treated at 1273 K for one week.

Magnetization data were measured by a SQUID magnetometer (MPMS; Quantum Design) between 5 and 300 K. Data were collected for zero field cooled (ZFC) samples on heating in a constant magnetic field of 4–80 kA m^{-1} and under field cooling (FC) conditions in a field of 8 or 80 kA m^{-1}. Magnetization data in high fields, $H \leq 4$ MA m^{-1}, were collected at 5–50 K.

Powder neutron diffraction data were collected with an OPUS IV two-axis diffractometer at the JEEP II

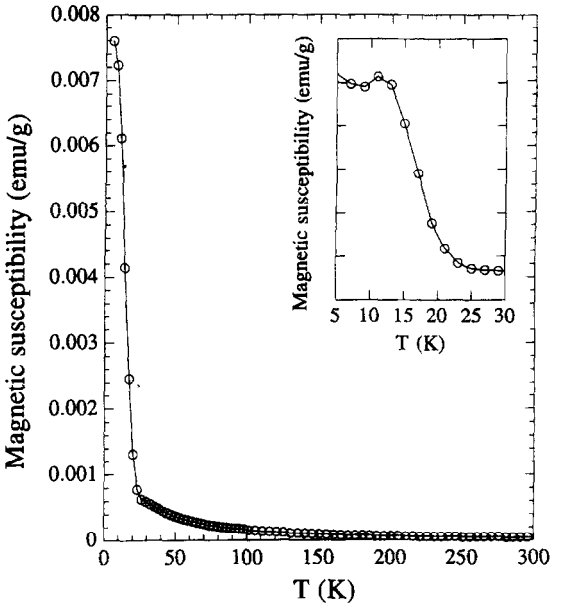

Fig. 1. Magnetic susceptibility of $Ca_3Co_2O_6$ at a field of 80 kA m^{-1} between 5 and 300 K. More detailed measurements in the region between 5 and 30 K are shown in the inset.

reactor, Kjeller. Cylindrical sample holders were used. Monochromatized neutrons of wavelength 182.5 pm were obtained by reflection from Ge(1 1 1). The scattered intensities were measured by five ^{3}He detectors, positioned ten degrees apart. Intensity data were collected from $2\Theta = 5$ to 100° in steps of $\Delta 2\Theta = 0.05°$. Low temperatures were obtained by means of a Displex

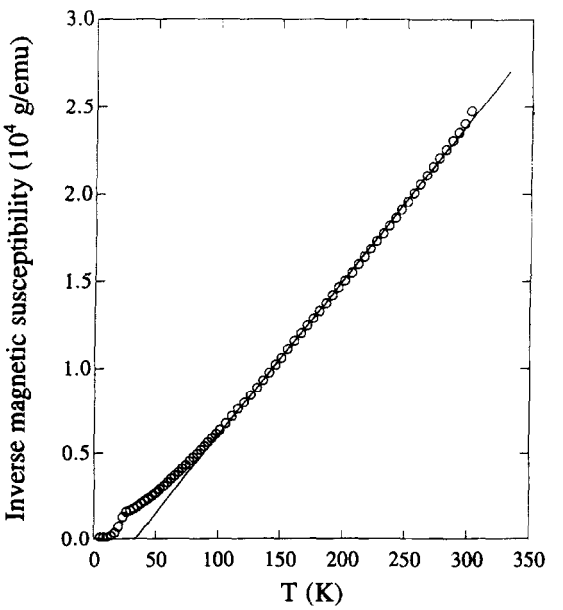

Fig. 2. Inverse magnetic susceptibility of $Ca_3Co_2O_6$ between 5 and 300 K measured in a field of 80 kA m^{-1}. The solid line is a linear fit to the data for $T > 80$ K.

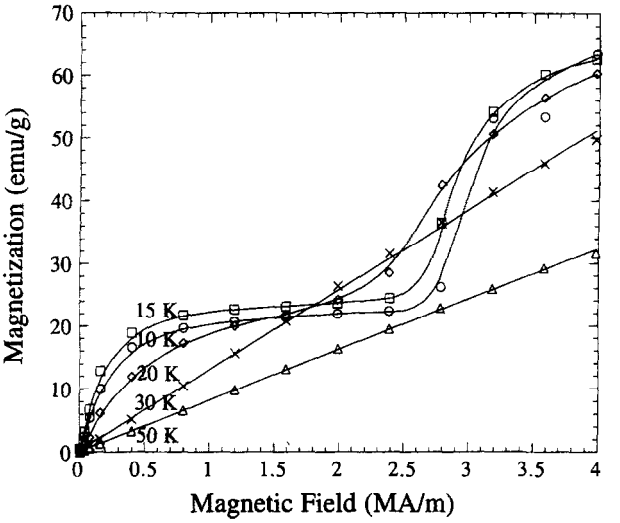

Fig. 3. Magnetization of $Ca_3Co_2O_6$ at between 10 and 50 K at magnetic fields between 800 A m^{-1} and 4 MA m^{-1}.

cooling system. A Lake Shore DRC 82C controller was used, and the temperature was measured and controlled by means of a silicon diode.

Structural and instrumental parameters were obtained from profile refinements. The Hewat version of the Rietveld program [5, 6] was used. The scattering amplitudes $b_{Ca} = 4.90$ fm, $b_{Co} = 2.50$ fm and $b_O = 5.803$ fm, and the form factors for Co^{2+} and Co^{3+} were taken from International Tables of Crystallography [7].

3. RESULTS AND DISCUSSION

3.1 *Magnetic characterization*

The magnetic susceptibility (FC) curve for $Ca_3Co_2O_6$ measured at a field of 80 kA m^{-1} is given in Fig. 1. No difference was observed in the magnetic susceptibility ZFC and FC curves, and also changing the magnetic field between 4 and 80 kA m^{-1} made no difference to the magnetic susceptibility curve shapes. A magnetic transition (T_{magn}) was observed at 24 ± 2 K and the susceptibility data could be fitted to a Curie–Weiss law [$\chi_g = C_g/T - \Theta$)] above 80 K as shown in Fig. 2. An effective magnetic moment $\mu_{eff} \approx (8 \cdot C_g \cdot M_w)^{1/2} = 5.7 \pm 0.2\,\mu_B$ and a paramagnetic Curie temperature $\Theta = 28 \pm 3$ K could be calculated from the linear fit to the inverse magnetic susceptibility.

Magnetization data for $Ca_3Co_2O_6$ measured between 10 and 50 K under increased magnetic fields from 800 A m^{-1} to 4 MA m^{-1} are shown in Fig. 3. A linear increase in the magnetization versus field is observed at $T \geq 30$ K data. At lower temperatures, a plateau is observed in the magnetization at around 22 emu g^{-1} (1.31 μ_B per $Ca_3Co_2O_6$ unit), followed by a further steep increase in the magnetization above 2.2–2.7 MA m^{-1}.

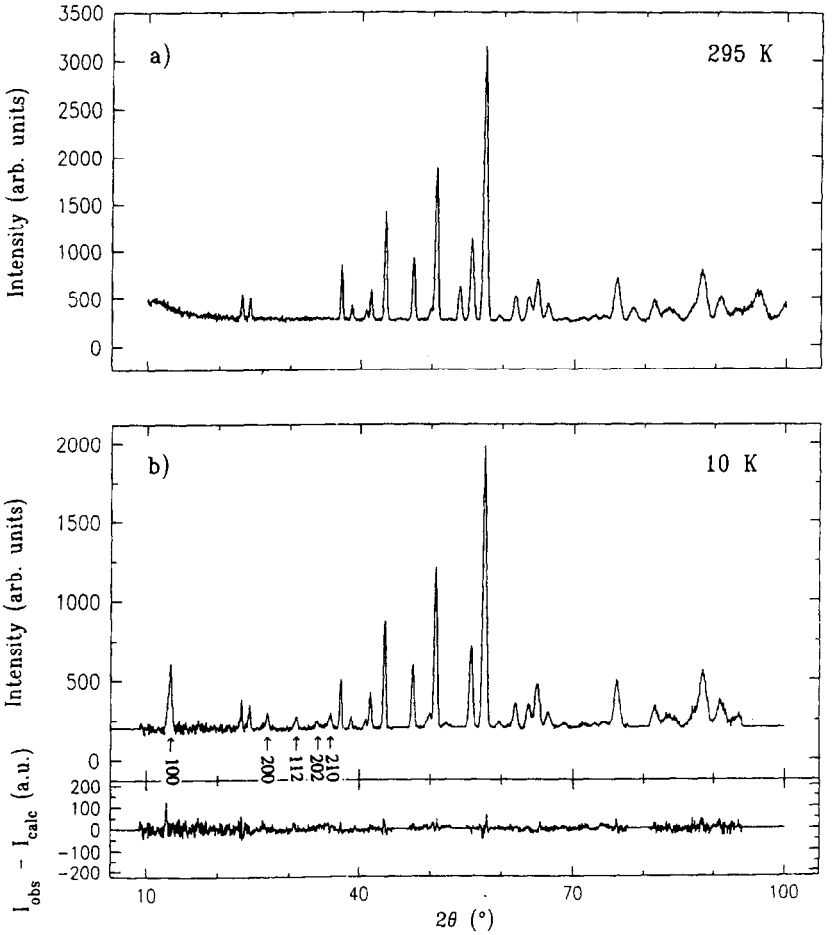

Fig. 4. Powder neutron diffraction diagrams for $Ca_3Co_2O_6$. Observed data at 295 K in (a) and observed and difference diagrams at 10 K in (b). Miller indices for the magnetic diffraction peaks and marked by arrows. Wavelength = 182.5 pm.

The rise of the saturation magnetization to the first plateau, is steepest at 15 K, notably less steep at 10 and 5 K (not shown). Complete saturation of the magnetization could not be obtained at magnetic fields ≤4 MA m^{-1}.

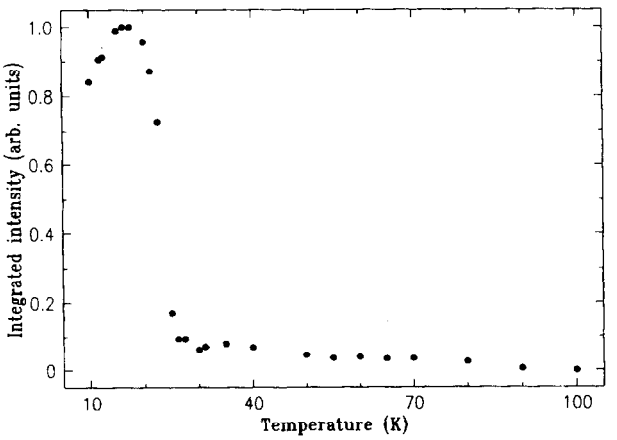

Fig. 5. Integrated intensity of the magnetic 1 0 0 reflection as function of temperature.

3.2 *Magnetic structure*

The magnetic structure of $Ca_3Co_2O_6$ was determined on the basis of powder neutron diffraction data at 10 K. $Ca_3Co_2O_6$ has previously been found to crystallize in space group $\underline{R\text{-}3c}$, $\underline{Z} = 6$ (hexagonal settings) at 298 K by powder X-ray and neutron diffraction data [3]. No changes in the neutron diffraction data were reported between 298 and 40 K [3]. The neutron diffractogram recorded at 10 K is compared to the 298 K data in Fig. 4. Five additional Bragg reflections ascribed to magnetic order appear at 10 K, indicating that an antiferromagnetic

Table 1. Observed magnetic ordering temperatures for $Ca_3Co_2O_6$, including Θ derived from the paramagnetic susceptibility

Temperature	T (K)
$T_{magn.}$ (SQUID)	24 ± 2
$T_{magn.}$ (Neutron diff.)	26 ± 2
Θ (Curie–Weiss law)	28 ± 3

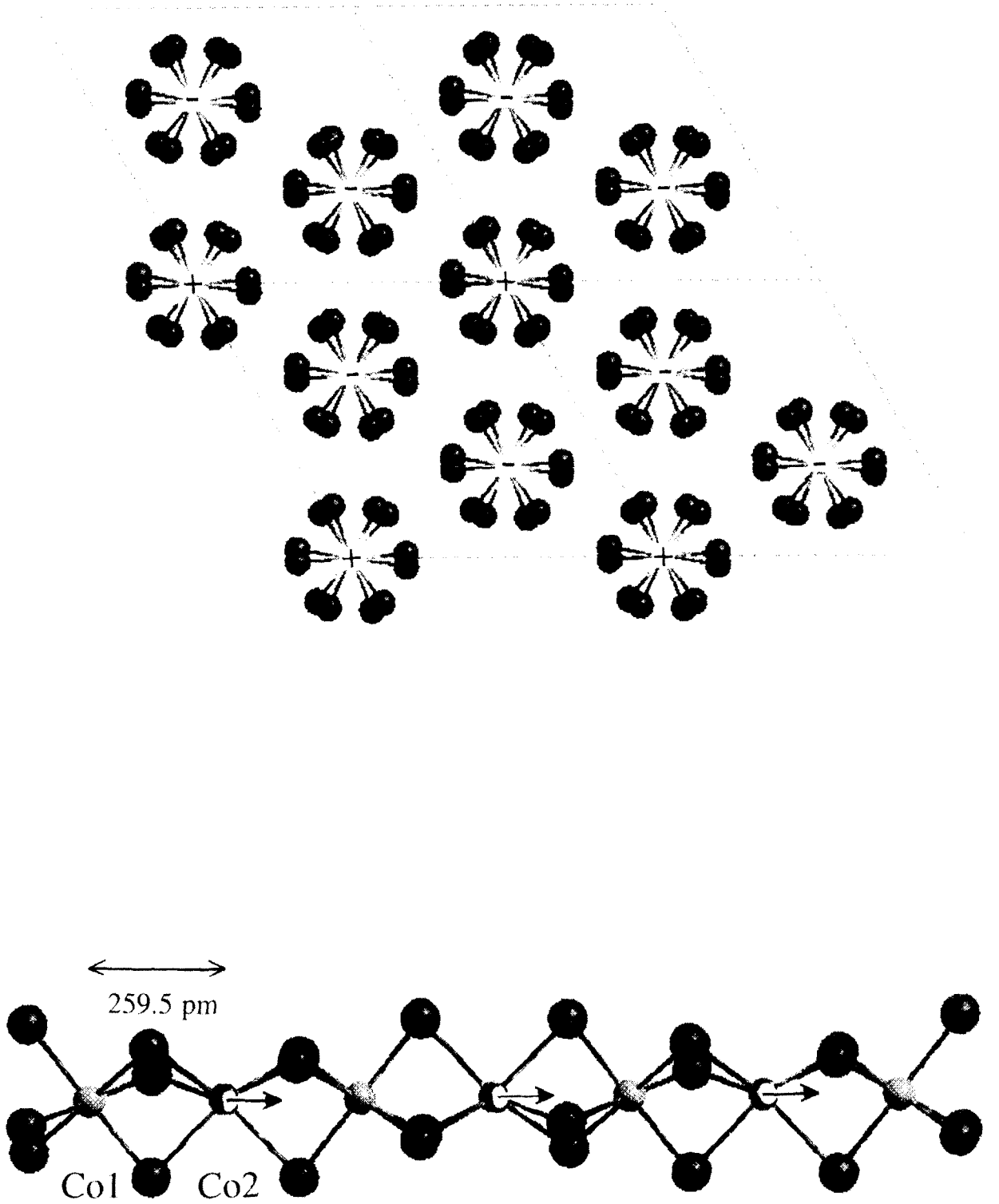

Fig. 6. The magnetic structure of $Ca_3Co_2O_6$. Upper projection on the **ab**-plane, lower, schematic illustration of one-dimensional chain (Ca atoms not shown).

ordering has occurred between 40 and 10 K. The magnetic diffraction peaks could be indexed on the hexagonal unit cell [**a** = 906.0(1) pm and **c** = 1036.23(9) pm] at 10 K, however, violating the rhombohedral extinction rules. The magnetic structure was therefore described in space group *P-3*, whereas parameters for the crystal structure were constrained as to correspond completely to the *R-3c* description. The magnetic ordering temperature,

Table 2. Atomic coordinates and unit cell dimensions for $Ca_3Co_2O_6$ (space group R-3c, see text) refined from powder neutron diffraction data at 10 K. Calculated standard deviations in parentheses. Temperature factors $B_{iso}(Ca) = 0.5(1)$, $B_{iso}(Co) = 0.0(2)$ and $B_{iso}(O) = 0.0(1)\ 10^4\ pm^2$

Atom	Site	x	y	z
Ca	18e	0.3705(4)	0	1/4
Co1	6b	0	0	0
Co2	6a	0	0	1/4
O	36f	0.1770(2)	0.0233(3)	0.1142(2)

a_H (pm)	906.0(1)
c_H (pm)	1036.6(1)
V_H (10^6 pm^3)	736.9(2)
R_N	3.28
R_M	10.76

$T_{magn} = 26 \pm 2$ K, was determined from the temperature dependence of the intensity (Fig. 5) of the magnetic 1 0 0 reflection at $2\Theta = 13.35°$ (Fig. 4). Very good conformity is seen between magnetic ordering temperatures determined from magnetic measurements and neutron diffraction as shown in Table 1.

The magnetic susceptibility data (Fig. 1) indicate ferromagnetic interactions below T_{magn}. Deviations from the Curie–Weiss behaviour occur already below 100 K. Combined with observed additional magnetic reflections at 10 K (Fig. 4) it is probable that $Ca_3Co_2O_6$ is ferrimagnetically ordered. The high relative intensity of the 1 0 0 magnetic reflection indicates the most of the magnetic moment is perpendicular to the **a**-axis (and **ab**-plane), hence lying along the **c**-axis, i.e. in the direction of the one-dimensional Co–O chains. Different magnetic models were tested out during Rietveld type refinements. A very simple model provided an excellent fit to the observed intensities [Fig. 4(b)]. Crystal data, atomic coordinates and R-factors from the refinement of the 10 K powder neutron diffraction data are given in Table 2. The magnetic structure is shown in Fig. 6. The Co–moments are aligned along [0 0 1] and ferromagnetic coupling dominates within the chains. A magnetic moment in the **c**-direction of $0.08 \pm 0.04\ \mu_B$ was refined for Co1, while a magnetic moment of $3.00 \pm 0.05\ \mu_B$ was refined for Co2. Attempts to consider small in-plane components of the magnetic moments were made, however no better fit to the data could be obtained. Introduction of a small ($1\ \mu_B$) magnetic moment for Co1 or Co2, did not give significantly worse fits ($R_N = 3.28$, $R_M = 11.8$ vs $R_N = 3.28$, $R_M = 10.8$). In one of the three Co–O chains in the hexagonal unit cell the cobalt atoms have magnetic spins up, while the Co atoms in the other two chains have spin down. Thus one third of the Co–O chains have all the six neighbouring chains antiferromagnetically coupled, while the other two Co–O chains have half the neighouring chains ferro- and antiferromagnetically coupled (Fig. 6).

Table 3. Magnetic moments for $Ca_3Co_2O_6$

Method	M per $Ca_3Co_2O_6$
Paramagnetic susceptibility	$\mu_{eff} = 5.7 \pm 0.2\ \mu_B$
Magnetization	$3 \times \mu_{plateau} = 3.9 \pm 0.2\ \mu_B$
PND refinement	$\mu_{Co1} = 0.08 \pm 0.04\ \mu_B$
	$\mu_{Co2} = 3.00 \pm 0.05\ \mu_B$

The steep increase in the magnetization vs magnetic field at around 2.7 MA m^{-1} (Fig. 3) indicates a field-induced phase transition from the ferrimagnetic to the ferromagnetic state of $Ca_3Co_2O_6$. Saturation of the ferromagnetic component of the ferrimagnetic structure may be assumed at the plateau in the magnetization vs magnetic field curve. From the proposed magnetic structure, a complete ferromagnetic saturation magnetism of three times the plateau value (around 66 emu g^{-1}) is expected. The extrapolated value of around $1.31\ \mu_B$ per $Ca_3Co_2O_6$ at the plateau then indicates a final magnetic moment of around $4\ \mu_B$ per $Ca_3Co_2O_6$. The calculated magnetic moment for $Ca_3Co_2O_6$ from the Rietveld refinement of the neutron data is somewhat lower. Experimental and magnetic moments for $Ca_3Co_2O_6$ are compared in Table 3.

Alternating octahedral (Co1) and trigonal prismatic (Co2) coordinated cobalt atoms exist along the one-dimensional Co–O chains in $Ca_3Co_2O_6$ [3]. Distinctly different Co–O distances are found for the two cobalt atoms, i.e. 191.6 pm for Co1–O and 206.2 pm for Co2–O [3]. The larger Co2–O distances indicate that the cobalt ions in the Co2 sites have larger ionic radius than in the

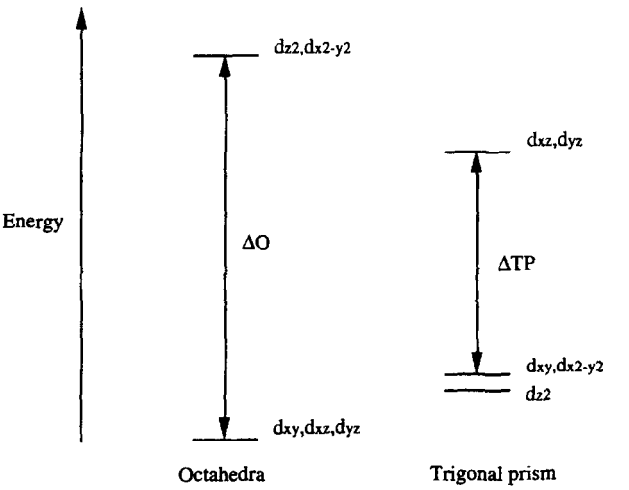

Fig. 7. Schematic illustration of the **d**-orbital energies for octahedral and a trigonal prismatic fields.

Co1 sites. Different sizes of the two cobalt ions are possible through charge ordering (Co^{4+} and Co^{2+}) and/or different spin configurations (low spin and high spin) for Co1 and Co2. From the calculated magnetic moments for Co1 ($0.08 \pm 0.04\ \mu_B$) and Co2 ($3.00 \pm 0.05\ \mu_B$), a low spin configuration for Co1 and a high spin configuration for Co2 is proposed. The energy levels of the transition metal **d**-orbitals in octahedral (O) and trigonal prismatic (TP) ligand fields are illustrated in Fig. 7. A lower energy gap is expected for the TP than for the O field, Δ_{TP} is approximately 2/3 Δ_O [8]. The proposed low spin configuration for the octahedrally coordinated Co1 and high spin for the trigonal prismatic coordinated Co2 is therefore in good agreement with expected ligand field energies.

The experimental results for the ordered magnetic moments, high-field magnetization at low temperatures and the paramagnetic moment for $Ca_3Co_2O_6$ should be considered in relation to several models. According to TGA the oxygen content in $Ca_3Co_2O_6$ is 5.97 [3]. Furthermore, refinements of the PND data show that the occupation number of oxygen does not differ significantly from one (completely filled site). This implies that the average formal oxidation state for cobalt is three. The models discussed below assume the orbital contribution to be quenched ($L = 0$; spin only), however, frequently this is not the case for cobalt. The two different coordination polyhedra for cobalt are first considered to be independent. At least three different situations can be envisaged.

(i) Co1 (Co^{III}_{oct}, low spin) and Co2 (Co^{III}_{trig}, high spin) with ordered magnetic moments of $0\ \mu_B$ and $4\ \mu_B$, respectively. The magnetic moment for Co2 is higher than calculated from the PND data.

(ii) Col (Co^{IV}_{oct}, low spin) and Co2 (Co^{II}_{trig}, high spin), giving ordered magnetic moments of $1\ \mu_B$ and $3\ \mu_B$, respectively. In this case, the magnetic moment for Co1 is too high compared with the PND results. The expected magnetic moments for both models (i) and (ii) are in good agreement with the high field magnetization data. However, the paramagnetic moments are lower than the observed value (Table 3).

(iii) Co1 (Co^{II}_{oct} and Co^{IV}_{oct}, low spin) and Co2 (Co^{III}_{trig}, high spin) giving average ordered magnetic moments of $1\ \mu_B$ and $4\ \mu_B$, respectively. These moments are higher than observed by PND data, however, in more close agreement with paramagnetic data than models (i) and (ii). Considering the face-sharing of the CoO_6-coordination polyhedra, the isolated models may not be appropriate. Hence, the last model (iv) modifies either of the models (i)–(iii) with metal–metal bonding interactions between the very close Co-neighbours in the chains (260 pm). This could imply delocalization and change the energy levels of Co1 (d_{xz}) and Co2 (dz^2) (Fig. 7). It should be mentioned that such short Co–Co distance also occur between face-shared polyhedra in Co_2O_3 (nonmagnetic insulator) [9]. Recently, extended Hückel calculations were performed for describing electronic and magnetic properties of the one-dimensional ABO_6 chains in Sr_3ABO_6 (A = Co, Ni; B = Pt, Ir) [10]. It was concluded that direct metal–metal (A–B) interactions are very small. For further evaluation of the proposed models for $Ca_3Co_2O_6$, similar calculations, or more complete bond structure calculations, are required.

4. SUMMARY

The crystal structure of $Ca_3Co_2O_6$ contains one-dimensional CoO_3-chains with alternating coordination polyhedra of trigonal prisms and octahedra. $Ca_3Co_2O_6$ is ferrimagnetically ordered below 24 ± 2 K (ferromagnetic order within the chains that are partly antiferromagnetically coupled). Alternating magnetic moments of $0.08 \pm 0.04\ \mu_B$ and $3.00 \pm 0.05\ \mu_B$ derived from neutron diffraction suggest very different electronic states for the two crystallographically non-equivalent Co-atoms. None of the proposed models fit completely the observed ordered magnetic moments, high field magnetization data or paramagnetic susceptibility. The possibility of charge ordering in addition to spin ordering (low-high spin) remains open.

Acknowledgements—Financial support from The Research Council of Norway is gratefully acknowledged.

REFERENCES

1. Brisi, C. and Rolando, P., *Ann. Chim. (Rome)*, **58,** 1968, 676.
2. Woermann, E. and Muan, A., *J. Inorg. Nucl. Chem.*, **32,** 1970, 1455.
3. Fjellvåg, H., Guldbrandsen, E., Aasland, S., Olsen, A. and Hauback, B.C., *J. Solid State Chem.*, in press.
4. Nguyen, T.N. and zur Loye, H.-C., *J. Solid State Chem.*, **117,** 1995, 300.
5. Rietveld, H.M., *J. Appl. Crystallogr.*, **2,** 1969, 65.
6. Hewat, A.W., *The Rietveld Computer Program for the Profile Refinement of Neutron Diffraction Powder Patterns Modified for Anisotropic Thermal Vibrations*, UKAERE Harwell Report RRL 73/897, 1973.
7. Wilson, A.J.C., *International Tables of Crystallography*, Vol. C, Kluwer Academic Publisher, Dordrecht, 1992.
8. Purcell, K.F. and Kotz, J.C., *Inorganic Chemistry*, Chap. **9 & 10**, Holt–Saunders International Editions, Japan, 1985.
9. Chenavas, J., Joubert, J.C. and Marezio, M., *Solid State Commun.*, **9,** 1971, 1057.
10. Vajenine, G.V., Hoffmann, R. and zur Loye, H.-C., *Chem. Phys.*, **204,** 1996, 469.